Neurobiology of Disease 65 (2014) 82–92

Contents lists available at ScienceDirect

Neurobiology of Disease

journal homepage: www.elsevier.com/locate/ynbdi

Spreading of amyloid-β peptides via neuritic cell-to-cell transfer is dependent on insufficient cellular clearance

Jakob Domert [a], Sahana Bhima Rao [a], Lotta Agholme [a], Ann-Christin Brorsson [b], Jan Marcusson [c], Martin Hallbeck [a,d], Sangeeta Nath [a,*]

[a] Pathology, Department of Clinical and Experimental Medicine, Faculty of Health Sciences, Linköping, Sweden
[b] Department of Physics, Chemistry and Biology, IFM, Linköping University, Linköping, Sweden
[c] Division of Geriatric Medicine, Department of Clinical and Experimental Medicine, Faculty of Health Sciences, Linköping University, Linköping, Sweden
[d] Department of Clinical Pathology, County Council of Östergötland, Linköping, Sweden

ARTICLE INFO

Article history:
Received 17 July 2013
Revised 9 December 2013
Accepted 30 December 2013
Available online 9 January 2014

Keywords:
Alzheimer's disease
Amyloid-β oligomers
Cell-to-cell transfer
Prion-like propagation
Intracellular accumulation

ABSTRACT

The spreading of pathology through neuronal pathways is likely to be the cause of the progressive cognitive loss observed in Alzheimer's disease (AD) and other neurodegenerative diseases. We have recently shown the propagation of AD pathology via cell-to-cell transfer of oligomeric amyloid beta (Aβ) residues 1–42 (oAβ_{1-42}) using our donor–acceptor 3-D co-culture model. We now show that different Aβ-isoforms (fluorescently labeled 1–42, 3(pE)-40, 1–40 and 11–42 oligomers) can transfer from one cell to another. Thus, transfer is not restricted to a specific Aβ-isoform. Although different Aβ isoforms can transfer, differences in the capacity to clear and/or degrade these aggregated isoforms result in vast differences in the net amounts ending up in the receiving cells and the net remaining Aβ can cause seeding and pathology in the receiving cells. This insufficient clearance and/or degradation by cells creates sizable intracellular accumulations of the aggregation-prone Aβ_{1-42} isoform, which further promotes cell-to-cell transfer; thus, oAβ_{1-42} is a potentially toxic isoform. Furthermore, cell-to-cell transfer is shown to be an early event that is seemingly independent of later appearances of cellular toxicity. This phenomenon could explain how seeds for the AD pathology could pass on to new brain areas and gradually induce AD pathology, even before the first cell starts to deteriorate, and how cell-to-cell transfer can act together with the factors that influence cellular clearance and/or degradation in the development of AD.

Introduction

Multiple lines of evidence have established that toxic aggregates and depositions of amyloid beta (Aβ) peptides play key roles in the pathology of Alzheimer's disease (AD; Hardy and Selkoe, 2002). Recent studies have found that the presence of soluble forms of Aβ oligomers correlates better with cognitive impairment and synaptic dysfunction than the presence of insoluble deposits (Brouillette et al., 2012; Selkoe, 2008). Experimental evidence has shown that soluble Aβ oligomers – both extracellular (Benilova et al., 2012) and intracellular (Gouras et al., 2010; LaFerla et al., 2007; Wirths et al., 2001) – play an important role in AD pathology. Neurotoxicity associated with intracellular accumulation of soluble Aβ oligomers has been reported as an early event in AD and may be responsible for synaptic dysfunction (Klein et al., 2001). These accumulations could come from either Aβ produced intracellularly (Wirths et al., 2001) or Aβ internalized from the extracellular space (Nath et al., 2012). The accumulation of intracellular Aβ can be transferred from one cell to a connected cell, which may lead to gradual pathological progression in AD (Nath et al., 2012). Similar prion-like propagation capacities have been suggested for other neurodegenerative proteins, such as α-synuclein and tau (Clavaguera et al., 2009; Desplats et al., 2009). The mechanisms involved in this transfer are not yet understood. However, these previous studies on cell-to-cell transfer with different neurodegenerative aggregates suggest that the endosomal–lysosomal pathway or the lysosomal exocytosis process may be involved in the transfer mechanism.

Aging is the main risk factor for sporadic AD; it is linked to the gradual dysfunction of the degradation systems, thus causing the cellular accumulation of various proteinaceous aggregates (Villeda et al., 2011). Reduced lysosomal and proteosomal degradation efficiencies have also been associated with AD progression because they may lead to intraneuronal accumulations of Aβ aggregates (Agholme et al., 2012; Nixon et al., 2008; Zheng et al., 2011). Additionally, defective Aβ-degrading enzymes and aberrant clearance processes of lipoproteins, ApoE, and low-density lipoprotein receptors play crucial roles in the

* Corresponding author. Fax: +46 10 1031529.
E-mail address: Sangeeta.Nath@liu.se (S. Nath).

0969-9961
http://dx.doi.org/10.1016/j.nbd.2013.12.019

AD etiology (Deane et al., 2008). These findings suggest that the decreased degradation and/or clearance of Aβ are involved in the toxic accumulation and cytotoxic effects.

Amyloid precursor protein (APP) can be cleaved and processed in several ways, resulting in Aβ variants that differ in length, cytotoxicity and proportion in the AD brain. Clinical studies have revealed the existence of a variety of toxic aggregates of different Aβ isoforms variably distributed as depositions in the AD brains (Benilova et al., 2012). Thus, we are interested in whether the reported differences in neurotoxicity between different Aβ isoforms could be related to their propensities for cell-to-cell transfer. Furthermore, we wanted to investigate whether this type of transfer was related to cytotoxicity or cellular degradation and/or clearance of Aβ. Intracellular accumulations of non-degradable toxic aggregates are important for neurotoxicity. Therefore, the role of cell-to-cell transfer in the disease progression and its relationship to cellular clearance and/or degradation may give fundamental clues to the etiology of AD. We compared four different Aβ species present in the AD brain to cover different parts of the large spectrum of Aβ variants. The most prevalent Aβ species in the brain is $Aβ_{1–40}$. Another variant, $Aβ_{1–42}$, is less abundant, but it is more cytotoxic; it is also aggregation-prone, and its proportion rises in the AD brain (Kuperstein et al., 2010). The toxicity of the N-terminal-truncated pyro-glutamate moiety-modified $Aβ_{3(pE)–40}$ isoform is almost comparable to the moderately toxic $Aβ_{1–40}$ isoform (Tekirian et al., 1999). The non-toxic, unmodified, N-terminal-truncated Aβ peptide $Aβ_{11–42}$ (Jang et al., 2010, 2013) was included as a negative control.

We show that oligomers of different fluorescently labeled Aβ-isoforms ($Aβ_{1–42;\ 1–40;\ 3(pE)–42;\ 11–42}$) can transfer from cell to cell. Although different Aβ isoforms can transfer between cells, the inability to clear and/or degrade more resistant isoforms, such as oligomeric $Aβ_{1–42}$ ($oAβ_{1–42}$), leads to larger net accumulations that could promote the cell-to-cell transfer. Furthermore, cell-to-cell transfer is an early event that is seemingly independent of later cellular toxicity. Together, these phenomena could explain how seeds for AD pathology could pass on to new brain areas and gradually induce the AD pathology before the first cell starts to die.

Methods

Labeling of Aβ peptides

The synthetic Aβ peptides $Aβ_{11–42}$ and $Aβ_{3(pE)–40}$ (Innovagen) were dissolved in 20 mM HEPES buffer, pH 7.4, and vortexed until completely dissolved. The solution was added to 6-carboxytetramethylrhodamine succinimidyl ester (TMR) (Invitrogen), an amine-reactive fluoroprobe, in a molar ratio of 2:1. The solution was vortexed and incubated overnight at 4 °C. After the incubation, the unbound dye was removed by size-exclusion chromatography using PD-10 columns (GE Healthcare). The samples were collected from the column, divided into small aliquots and freeze-dried. The freeze-dried samples were re-suspended in 1,1,1,3,3,3-hexafluoro-2-propanol (HFIP) and freeze-dried; then, they were stored at −20 °C. The synthetic $Aβ_{1–42}$ and $Aβ_{1–40}$ peptides labeled with TMR (AnaSpec) were divided into small aliquots by re-suspension in HFIP and stored at −20 °C following freeze-drying. The labeling percentages were calculated by measuring the concentration of TMR at an absorbance wavelength of ~550 nm (TMR $\varepsilon_{555nm} = 65{,}000\ M^{-1}\ cm^{-1}$ (Haugland, 2001)) and comparing the concentration with the amount of total protein measured using a Bio-Rad protein assay kit. The percentages of fluoroprobe TMR labeling for the $oAβ_{(1–42;\ 1–40;\ 3(pE)–42;\ 11–42)}$-TMR peptides were 23.8%, 7.5%, 3.5% and 5.3%, respectively.

Preparation of oligomers and protofibrils

To obtain oligomers from the freeze-dried peptides, the lyophilized Aβ variants were dissolved in dimethyl sulfoxide (DMSO) to 1.5 mM and immediately vortexed. Then, the solution was diluted to 100 μM using 20 mM HEPES buffer and sonicated for 2 min. The sonicated samples were incubated at 4 °C for 24 h, causing the formation of oligomers (Nath et al., 2012).

Protofibrils were prepared using a standard characterized protocol (Klingstedt et al., 2011). $Aβ_{1–42}$-TAMRA was dissolved in 2 mM NaOH to a concentration of 222 μM. Then, the sample was diluted in PBS to a final concentration of 10 μM and incubated at 37 °C for 7 h.

Transmission electron microscopy (TEM)

Transmission electron microscopy (TEM) was used to characterize the prepared oligomers. The prepared Aβ oligomers (oAβ) of the respective variants ($Aβ_{1–42;\ 1–40;\ 3(pE)–42;\ 11–42}$) were diluted to 10 and 30 μM in HEPES buffer and were added to carbon-coated nickel grids, which were incubated for 1 min and blotted with filter paper. The samples were incubated with 10 μl of 2% uranyl acetate for 15 s for negative staining; the grid was then dried using filter paper. The prepared sample grids were viewed in a JEOL 1230 transmission electron microscope (Jeol Ltd; Tokyo, Japan), and the images were captured with ORIUS SC 1000 CCD camera.

Differentiation and co-culturing of SH-SY5Y cells

The SH-SY5Y (ECACC; Sigma Aldrich) donor cells were differentiated as described earlier (Agholme et al., 2010; Nath et al., 2012) using 10 μM retinoic acid (RA; Sigma Aldrich). The donor cells were incubated with either 500 nM or 1 μM of the oAβ-TMR peptides for 3 h at 37 °C. The cells were then washed twice with PBS for 10 min at 37 °C, trypsinized, mixed (75,000–100,000 cells) with pre-chilled extracellular matrix (ECM) gel (Sigma Aldrich) at a 1:1 ratio and reseeded. The highly differentiated SH-SY5Y acceptor cells were cultured in ECM gel and differentiated with media that included brain-derived neurotropic factor (BDNF), neuregulin β1 (NRGβ), nerve growth factor (NGF) and vitamin D3 (Agholme et al., 2010). After 10 days of differentiation, the cells were transfected with EGFP-tagged endosomal (Rab5a) or lysosomal (lysosomal-associated membrane protein 1, LAMP-1) proteins using Organelle Lights BacMam-2.0 (Invitrogen) (Nath et al., 2012).

The donor and acceptor cells were co-cultured by adding 75,000 donor cells in ECM gel to 80,000 differentiated acceptor cells on chambered glass slides and incubating them in RA supplemented MEM media for 24, 48 or 72 h at 37 °C (Nath et al., 2012). The cells were fixed using 4% paraformaldehyde and mounted using ProLong gold anti-fade mounting media (Invitrogen) after 24, 48 or 72 h of incubation. Cell-to-cell transfers also were studied after the addition of 50 nM rapamycin (Fisher Scientific) in the co-culture media for 24, 48 or 72 h at 37 °C.

Confocal microscopy

Images of fixed cells and live cells were taken using a LSM 700 Zeiss confocal microscope. The differential interface contrast (DIC) mode and the red and green channels were used to take the images with 40× oil plan-apochromatic DICII objectives. Transmitted light was used for DIC, and 543 nm and 488 nm laser excitation wavelengths were used to image the red and green channels, respectively.

Analysis of late-endosomal or lysosomal co-localization and degradation of oligomers

The partially differentiated (10 μM RA for 7 days) SH-SY5Y cells were incubated with 500 nM of the respective oligomeric Aβ-TMR variant, diluted in P/S (penicillin/streptomycin) and supplemented MEM media for 3 h at 37 °C. The cells were extensively washed with PBS (2 × 10 min at 37 °C) and incubated with 200 nM lysotracker green DND-26 (Invitrogen) for 15 min. Live-cell imaging using confocal microscopy was performed to determine the amount of internalized

oligomers and their co-localization to late-endosomes or lysosomes using the Volocity software (Perkin Elmer).

For degradation analysis, the cells were exposed to the different oAβ-TMR variants for 3 h, as described above, and were reseeded on chambered glass slides with ECM gel (80,000 cells/well). The cells were fixed and mounted after 24, 48 or 72 h of culturing. The areas of red fluorescent oligomers per cell were analyzed from confocal micrographs by averaging the area from at least 250 cells for each set and using Volocity software to determine the degradation of the internalized oligomers.

The calculated absolute areas of internalized red oligomers per cell at 0 h for the oAβ-TMR (1–42, 1–40, 3(pE)–40, 11–42) isoforms were 19.34 ± 0.22, 9.98 ± 0.12, 1.07 ± 0.02 and 2.48 ± 0.04 μm^2/cells, respectively. The calculated residual intracellular oligomers over time were normalized as percentages, considering the areas at 0 h as 100%.

Size exclusion chromatography (SEC)

The size exclusion chromatography (SEC) technique was used to separate monomers, dimers and higher oligomers from the prepared $A\beta_{1-42}$TMR oligomer solution. This solution (100 μM) was separated using a Superdex 75 10/300 GL column (GE Healthcare) equilibrated in PBS. After protein separation, 500 μl of each fraction was collected. The areas of the peaks were calculated to obtain quantitative data of the separated oligomers, dimers and monomers.

Western blot analysis of LAMP-2 expression

The donor cells were prepared from partially differentiated cells (10 μM RA for 7 days). The cells were incubated with 1 μM of each oAβ isoform for 3 h and reseeded into a 24-well plate for culturing with RA medium. The donor cells (100,000) that were internalized with 1 μM of each oAβ isoform after 24, 48 or 72 h of incubation were lysed in 0.5 M Tris HCl pH 6.8, which included 1% glycerol and 0.2% SDS. Cell lysates lacking Aβ were used as controls. Western blots were performed on the lysed protein samples by loading 10 μg of the samples into a 4–20% SDS ClearPage gels and using the mouse anti-human LAMP-2 antibody (SouthernBiotech), which was used at a 1:1000 dilution with blocking solution (5% non-fat dry milk). Goat anti-mouse HRP (Dako) was used at a 1:3000 dilution as a secondary antibody. The loading control was glyceraldehyde 3-phosphate dehydrogenase (GAPDH), and anti-GAPDH horseradish peroxidase (HRP) antibody (Novus Biologicals) was used in a 1:30,000 dilution.

Cytotoxicity assay and mitochondrial potential measurements with donor cells

Cell viability assays using XTT (2,3-bis [2-methoxy-4-nitro-5-sulfophenyl]-5-[(phenylamino) carbonyl]-2H-tetrazolium hydroxide) and measurements of mitochondrial potential using JC-1 were performed on the donor cells that had internalized 1 μM of either oAβ isoform after 24, 48 or 72 h of incubation. Cells lacking Aβ were used as controls.

The donor cells were added with XTT reagent and electron couple reagent (Roche) at a ratio of 50:1 to the media after 24, 48 or 72 h of reseeding. The reduced XTT product produced by mitochondrial enzymes in viable cells, formazan (bright orange in color) was measured after 8 h of incubation at 450 nm and 750 nm using a Victor Wallac (PerkinElmer) plate reader (Roehm et al., 1991; Scudiero et al., 1988).

The donor cells were incubated for 10 min with 5 μM JC-1 (Invitrogen) enriched serum free medium for the mitochondrial potential assay. Subsequent to the JC-1 incubation, the cells were washed twice in PBS and trypsinized. The cells were then resuspended in ice-cold PBS and filtered through a 30-μm mesh. The cells were briefly vortexed and then directly analyzed using a Calibur flow cytometer (equipped with a 488–514 nm argon laser) and the CellQuest Pro software (Becton Dickinson).

Statistical analysis

The data from the area analysis were expressed in the means ± SEM (standard errors of the mean) to represent the vast variation of the accumulated areas of the oligomers and the lysosomes. The other data were represented by the means ± SD (standard deviations). Hypothesis tests were calculated using a two-tailed unpaired Student's t-tests for the size distribution of lysosomes or one-way analyses of variance (ANOVAs) for evaluation of co-localization; the significance level was $p < 0.05$. Pearson's correlation was used for correlation analysis using GraphPad Prism software. Each batch of cell cultures represented one independent experiment ($n = 1$).

Results

Characterization of the oAβ isoforms

The prepared oligomers of the Aβ-TMR (1–42, 1–40, 3(pE)–40 and 11–42) isoforms were characterized. The TEM images showed that the samples consisted primarily of spherical oligomers (Fig. 1) without fibrils or proto-fibrils. The aggregation-prone $A\beta_{1-42}$TMR isomer formed larger oligomers of average diameter 42 ± 27 nm (Fig. 1A) compared to the oligomers of the relatively less aggregation-prone Aβ-TMR isoforms (1–40, 3(pE)–40 and 11–42) which had an average diameter of 24 ± 9 nm (Figs. 1B–D). Size exclusion chromatography (SEC) separation using Superdex 75 10/300 GL confirmed the formation of oligomers for all four isoforms. The oligomers of the respective isoforms were eluted at the void volume (MW > 70,000 Da) during the separation. The TMR fluorescence tags on the Aβ isoforms had no significant effects on oligomerization. In accordance with our previous data, oligomer formation and toxicity were similar compared to unlabeled $oA\beta_{1-42}$ samples (Nath et al., 2012).

Cell-to-cell transfer of oligomeric Aβ-isoforms

The cell-to-cell transfer properties of the different oAβ-TMR isoforms were compared using the same donor–acceptor co-culturing method (Fig. 2A) as in previous studies (Nath et al., 2012). All of the investigated isoforms transferred, with very different net amounts. The results revealed that the $oA\beta_{1-42}$TMR and $oA\beta_{3(pE)-40}$TMR isomers were transferred from the donor cells to the connected green acceptor cells, resulting in a considerable net amount (Fig. 2B). However, only a few of the connected acceptor cells (<5%) co-cultured with the $oA\beta_{1-40}$TMR- and $oA\beta_{11-42}$TMR-containing donor cells showed low-intensity, discrete red fluorescent spots that were distinguishable from auto-fluorescence (Fig. 2B). The presence of transferred red oligomeric isoforms in the acceptor cells that were connected to donor cells was quantified by counting several confocal images (at least 10 from each set) (Fig. 2C). The percentage of connected acceptor cells with transferred $oA\beta_{1-42}$TMR increased with time of incubation, while $oA\beta_{3(pE)-40}$TMR started to decrease at 72 h, following an initial increase at 48 h. The results suggest that transfer is not specific to any one Aβ isoform. All of the examined isoforms can transfer from donor cells to acceptor cells; however, the more aggregation-prone isoform $oA\beta_{1-42}$TMR caused large intracellular accumulations in the acceptor cells.

Degradation and/or clearance of oAβ-TMR isoforms and concomitant variation in cell-to-cell transfer

The disappearance of the internalized oAβ-TMR isoforms was analyzed over time using oAβ-TMR-fed donor cells incubated with the different oAβ-TMR isoforms and then extensively washed and reseeded. The 0 h donor cells were collected immediately after the oAβ-TMR

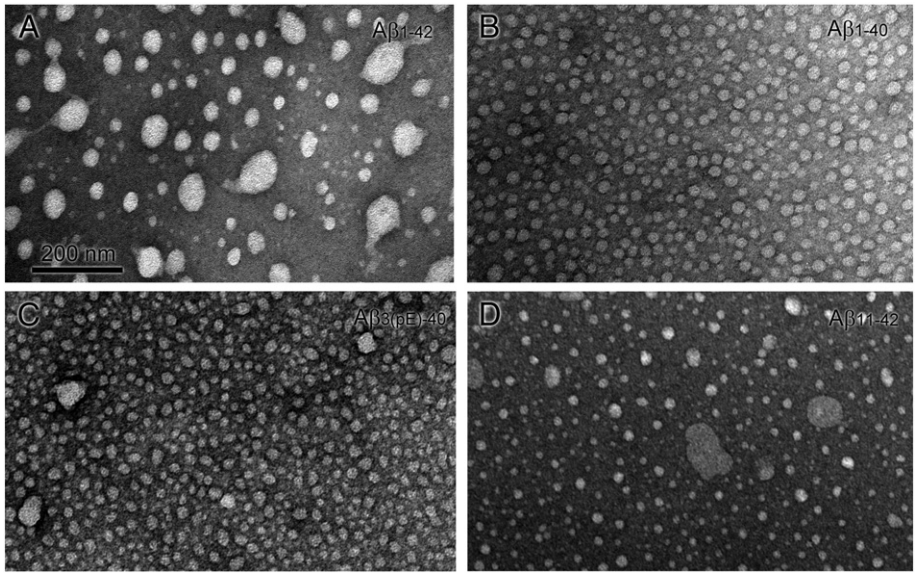

Fig. 1. Characterizations of oAβ isoforms. (A–D) Transmission electron microscopy (TEM) images show that (A) $A\beta_{1-42}$TMR, (B) $A\beta_{1-40}$TMR, (C) $A\beta_{3(pE)-40}$TMR and (D) $A\beta_{11-42}$TMR form mainly spherical oligomers during oligomer preparation. No fibrils were detected by EM. The aggregation-prone $A\beta_{1-42}$TMR isoform showed formation of larger-sized oligomers compared to the relatively less aggregation-prone $A\beta_{(1-40,\ 3(pE)-40,\ 11-42)}$TMR isoforms. A layer of oligomers was applied on a copper grid using 10 μl of 10 μM solutions of $A\beta_{1-42}$TMR and $A\beta_{1-40}$TMR. For the $A\beta_{3(pE)-40}$TMR and $A\beta_{11-42}$TMR isoforms, 10 μl of 30 μM solutions was used. Scale bars A = B = C = D = 200 nm; n = 3.

incubation to reflect the amount of initially internalized oligomers. The areas of internalized red oligomers per donor cell after 0, 24, 48 and 72 h were analyzed from confocal images (Fig. 3A) using the Volocity software to obtain the intracellular accumulations of the oAβ-TMR isoforms over time (Fig. 3B). The results revealed that only 10% of the internalized $oA\beta_{1-42}$TMR isoform had disappeared after 72 h. However, the cells managed to degrade and/or clear 53% of $oA\beta_{3(pE)-40}$TMR after 72 h of incubation. The isoforms $oA\beta_{1-40}$TMR and $oA\beta_{11-42}$TMR almost disappeared completely relative to the above two isoforms: 96% of $oA\beta_{1-40}$TMR and most of $oA\beta_{11-42}$TMR were cleared even before 48 h (Fig. 3B). Both degradation (Nixon et al., 2008) and clearance (Deane et al., 2008) have been described as mechanisms for expunging Aβ, and both mechanisms have been suggested to be involved in AD etiology. Further studies will be needed to clarify which of these mechanisms are responsible for the currently described reduction of Aβ oligomers.

The percentage of intracellularly accumulated oligomer for each isoform had a highly significant, linear Pearson's correlation ($r = 0.889$, $p = 0.001$) with the amount of cell-to-cell transfer over time (Fig. 3C). The highly significant linear correlation suggests that the inability to clear and/or degrade oAβ and subsequent intracellular accumulations could enhance the net amount of cell-to-cell transfer. The isoform $oA\beta_{1-42}$TMR showed abnormal intracellular accumulations and considerable cell-to-cell transfer over time compared to $oA\beta_{3(pE)-40}$TMR, $oA\beta_{1-40}$TMR and $oA\beta_{11-42}$TMR, which were more readily cleared and/or degraded by cells. It is plausible that these intracellular accumulations of $oA\beta_{1-42}$TMR promote cell-to-cell transfer, compared to $oA\beta_{3(pE)-40}$TMR, $oA\beta_{1-40}$TMR and $oA\beta_{11-42}$TMR isoforms which are less prone to accumulate intracellularly.

The involvement of lysosomal degradation was further investigated using rapamycin, an autophagy inducer. These experiments show lower accumulation (near significance at 48 h, significant at 72 h) and a tendency to decrease cell-to-cell transfer (not reaching statistical significance) of $oA\beta_{1-42}$TMR in the presence of 50 nM rapamycin compared to control (without rapamycin) over days (Figs. 3D–E). The transfer to the acceptor cell is secondary to the accumulation in the donor cells. Since the non-toxic level of rapamycin only results in a partial lower accumulation of $oA\beta_{1-42}$TMR in the donor cells, any change in the cell-to-cell transfer is expected to be small. However, the trend towards decreased oAβ transfers seen after rapamycin treatment supports a role of the lysosomal system in the net amount of cell-to-cell transfer.

Intracellular internalization of oAβ-TMR isoforms and their co-localization within late-endosomes/lysosomes

Previous studies have shown that oligomers of $A\beta_{1-42}$ and $A\beta_{1-40}$ spontaneously internalize and accumulate in the late-endosomal/lysosomal vesicles after extracellular administration (Hu et al., 2009; Nath et al., 2012). The intracellular internalization and co-localization in late-endosomes/lysosomes of extracellularly applied oAβ-TMR isoforms was analyzed after 3 h of incubation using live-cell confocal microscopy (Fig. 4A). The accumulation of oligomers in late-endosomes/lysosomes was quantified by determining the percentage of co-localization using both the overlap coefficient and global Pearson's correlation between the red fluorescent oAβ-TMR isoforms and the green lysotracker-labeled vesicles with Volocity software (Fig. 4B). The results from a one-way ANOVA test revealed that there was no significant difference ($p > 0.05$) in the percentage of co-localization of oligomers with lysotracker between the four different oAβ-TMRs. However, $oA\beta_{1-42}$TMR caused abnormal intracellular accumulation in donor cells and extra-large late-endosomal/lysosomal vesicles over time. Such vesicle structures were not observed after incubation with $oA\beta_{3(pE)-40}$TMR, $oA\beta_{1-40}$TMR or $oA\beta_{11-42}$TMR, which could be cleared with time (Fig. 4C).

Abnormal lysosomal morphology in $oA\beta_{1-42}$-TMR accumulated cells

Several studies have described the failure of the lysosomal degradation pathway in Aβ-peptide-associated AD pathology (reviewed in Nixon et al. (2008)). The accumulation of non-degradable Aβ peptides and abnormal lysosomal morphology in the axonal compartment has also been reported (Lee et al., 2011b). In the present study, the donor and acceptor cells with internalized $oA\beta_{1-42}$TMR exhibited larger lysosomes over time (Figs. 4C, 5A). The sizes of the $oA\beta_{1-42}$TMR-accumulated lysosomal vesicles in the acceptor cells suggest pathological changes following cell-to-cell transfer. Therefore, the changes in lysosomal areas (EGFP-tagged green lysosomal LAMP-1 protein) over time were determined by comparing the sizes before transfer (considered to be 0 h) and after oAβ-TMR transfer in acceptor cells. The vesicles were segregated into small (0–0.75 μm^2), medium (0.76–1.50 μm^2), large (1.51–5 μm^2) and extra-large vesicles (>5 μm^2) based on the standard areas of lysosomes (Bains and Heidenreich, 2009). There was a significant

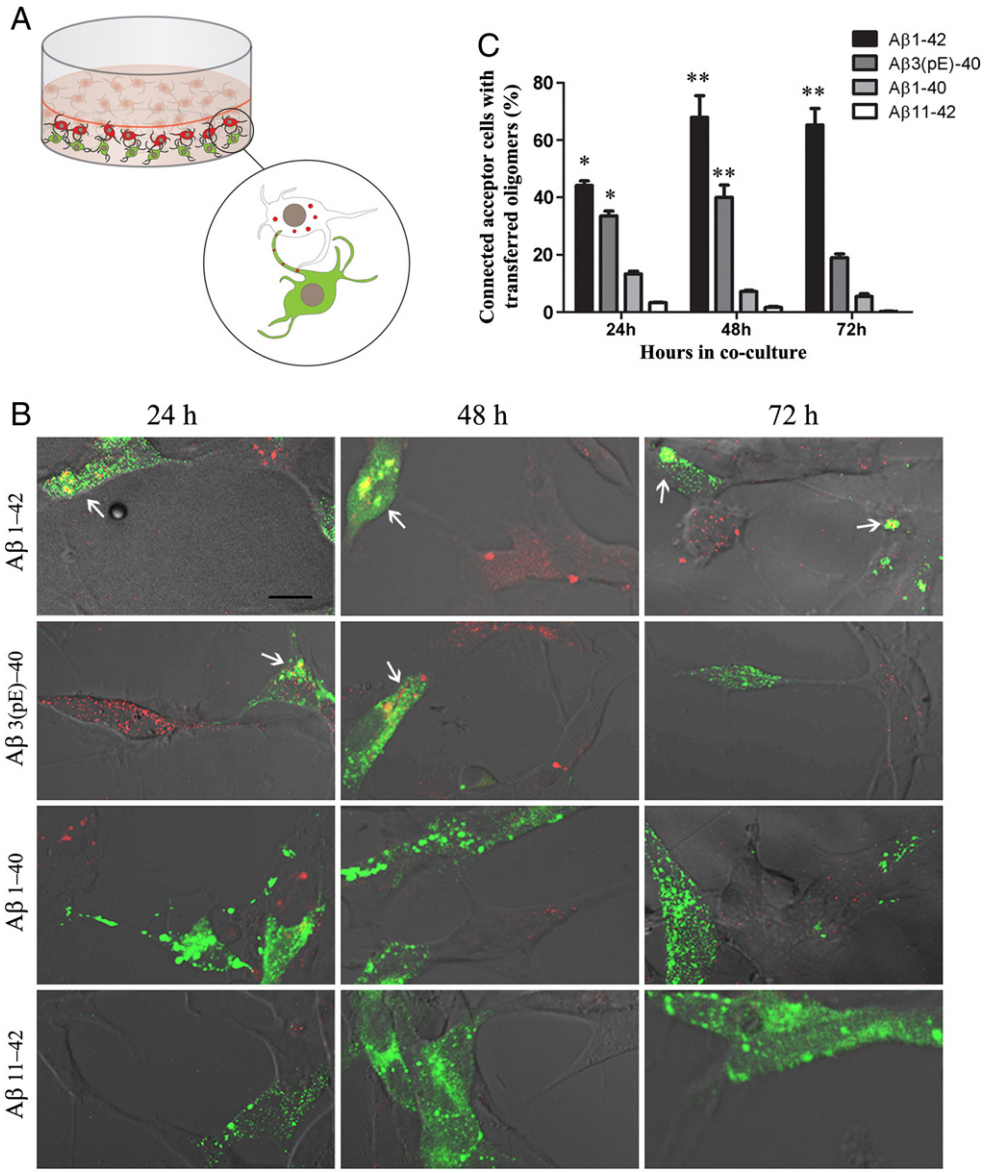

Fig. 2. Cell-to-cell transfer of oligomeric Aβ isoforms. (A) A cartoon illustrating the 3D co-culture model with differentiated SH-SY5Y cells employed to measure the transfer of the TMR-tagged red fluorescent Aβ peptides (1–40, 3(pE)–40, 11–42 and 1–42). The co-culture model consists of two cell populations seeded in ECM gel, in which one population has internalized red Aβ-TMR conjugates (donor cells) while the other expresses green GFP-tagged endo/lysosomal proteins (acceptor cells), allowing us to detect positive transfer between the two. (B) Superimposition of red, green and DIC confocal images shows the transfer of oAβ isoforms (red) between the donor cells (internalized with 500 nM oAβ isoforms) and the connected acceptor cells (green). Arrows indicate the transferred oligomers in the acceptor cells connected to donor cells. Scale bar = 10 μm. (C) Quantification of the connected acceptor cells with successfully transferred Aβ isoforms over time. Significantly higher numbers of acceptor cells were observed to contain $oA\beta_{1-42}$ and $oA\beta_{3(pE)-40}$ isoforms compared to cells with $oA\beta_{1-40}$ and $oA\beta_{11-42}$ isoforms. Data are represented as the means ± SD; n = 4.

increase in the number of extra-large vesicles after 48 h of $oA\beta_{1-42}$TMR transfer compared to the vesicle sizes detected at 0 h (Fig. 5B). The mean area of lysosomal vesicles was also significantly increased over time in acceptor cells containing transferred $oA\beta_{1-42}$TMR (Fig. 5C). A significant number of lysosomes with accumulated red fluorescent oligomers showed abnormal morphology and vesicle areas greater than 20 μm^2 (Fig. 5A). The lysosomes did not show any prominent changes in their structures when exposed to the less aggregation-prone oAβ isoforms (1–40 and 11–42) (data not shown). After exposure to the moderately degradable isoform $oA\beta_{3(pE)-40}$, medium- and large-sized vesicles appeared over time (Fig. 5A), but no significant change in the number of extra-large-sized lysosome vesicles was observed (data not shown). Similarly, abnormal accumulation-associated increases in the size of late endosomes/lysosomes were observed in the donor cells that had internalized $oA\beta_{1-42}$TMR (Fig. 4C).

The accumulation of the toxic oligomers of $A\beta_{1-42}$ can activate different autophagy pathways (Nixon et al., 2008). Furthermore, autophagy-associated lysosomal protein LAMP-2 activity has also been reported to increase under different stress conditions, including oxidative stress, prolonged starvation or exposure to toxic compounds (Cuervo and Dice, 2000; Saftig and Eskelinen, 2008). Hence, the LAMP-2 expression levels were studied over time in relation to the accumulation of non-degradable oAβ-TMR isoforms, particularly $oA\beta_{1-42}$TMR. Quantification by Western blot revealed a significant increase in LAMP-2 protein 72 h after $oA\beta_{1-42}$TMR internalization in donor cells (Fig. 5D). Separation of the acceptor cells receiving transfer from the co-culture is technically difficult, and abnormal lysosomes were evident in $oA\beta_{1-42}$TMR-treated donor and acceptor cells over time (Figs. 4C and 5A). Therefore, LAMP-2 quantifications were performed with donor cells. Other oAβ isoforms (3(pE)–40, 1–40 and 11–42) did not show any significant LAMP-2

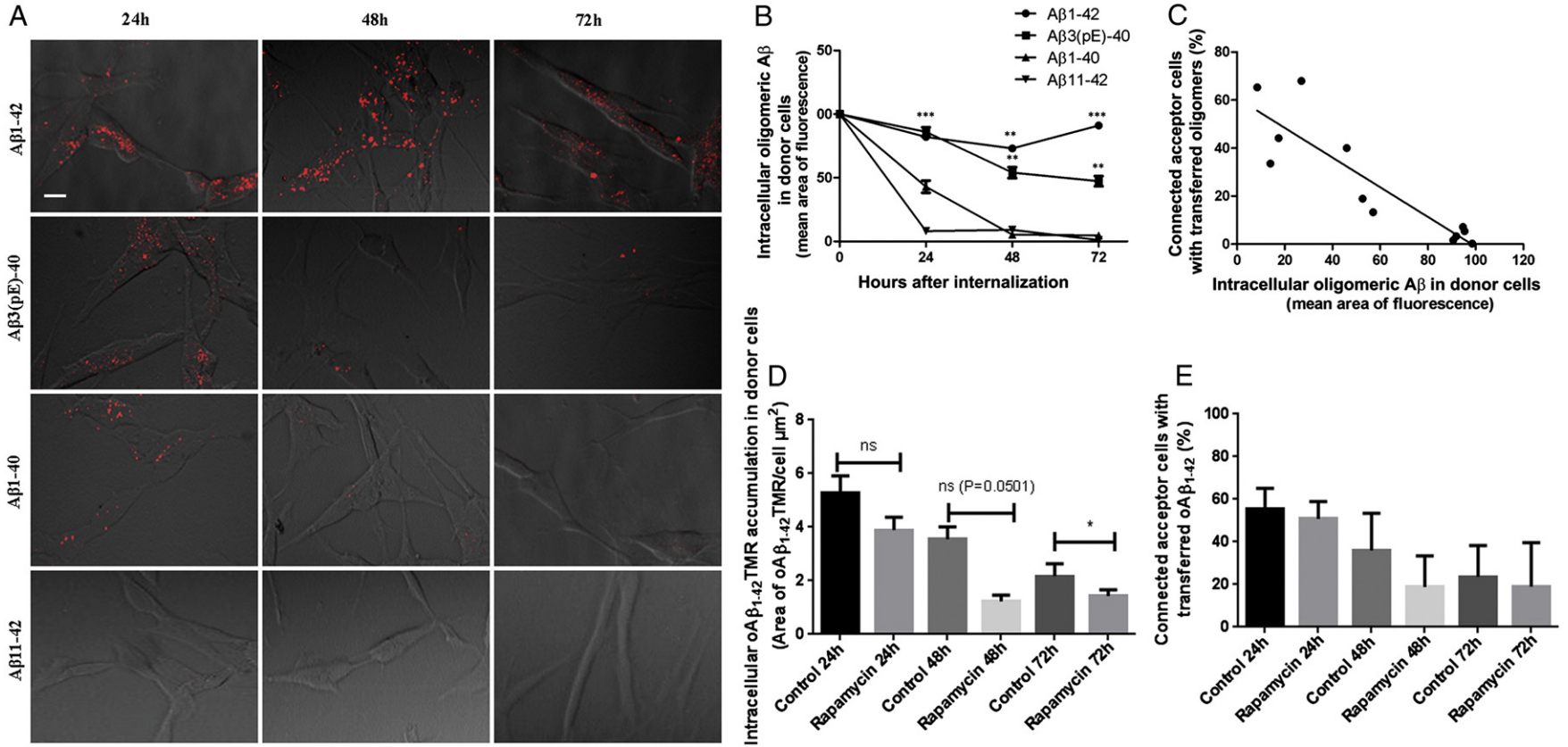

Fig. 3. Degradation of internalized oligomeric Aβ-isoforms. (A) Confocal images show residual oAβ-TMR isoforms (red) 24, 48 and 72 h after internalization. Donor cells were incubated with 500 nM oAβ-TMR isoforms for 3 h for oligomer internalization. Scale bar = 10 µm; n = 4. (B) Analysis of the confocal images using Volocity software revealed that $A\beta_{1-42}$ exhibited the greatest resistance (significantly higher compared to $A\beta_{11-42}$) to clearance and/or degradation, followed by $A\beta_{3(pE)-40}$, while $A\beta_{1-40}$ and $A\beta_{11-42}$ were almost completely cleared and/or degraded at 24 and 48 h, respectively. Data were calculated from ~250 cells for each isoform and are represented as the means ± SEM; n = 4. (C) When comparing the numbers of acceptor cells with transferred Aβ isoforms at 24, 48 and 72 h with corresponding residual internalized oligomers in donor cells, an inverse correlation was revealed (Pearson's correlation coefficient, r = −0.889, p = 0.001). (D) Analysis of $oA\beta_{1-42}$ in donor cells shows a decrease of accumulation with rapamycin (50 nM) compared to without. Data were analyzed from confocal images of ~250 cells for each data point and are represented as the means ± SEM; n = 2. (E) Cell-to-cell transfers of $oA\beta_{1-42}$ were quantified counting the connected acceptor cells with successfully transferred $oA\beta_{1-42}$ over time. There is a trend towards decreased net amount of $oA\beta_{1-42}$ but this did not reach statistical significance. Data represented as the means ± SD; n = 2. Statistical significance was evaluated using a two-tailed unpaired Student's *t* test. *p < 0.05, **p < 0.01 and ***p < 0.001.

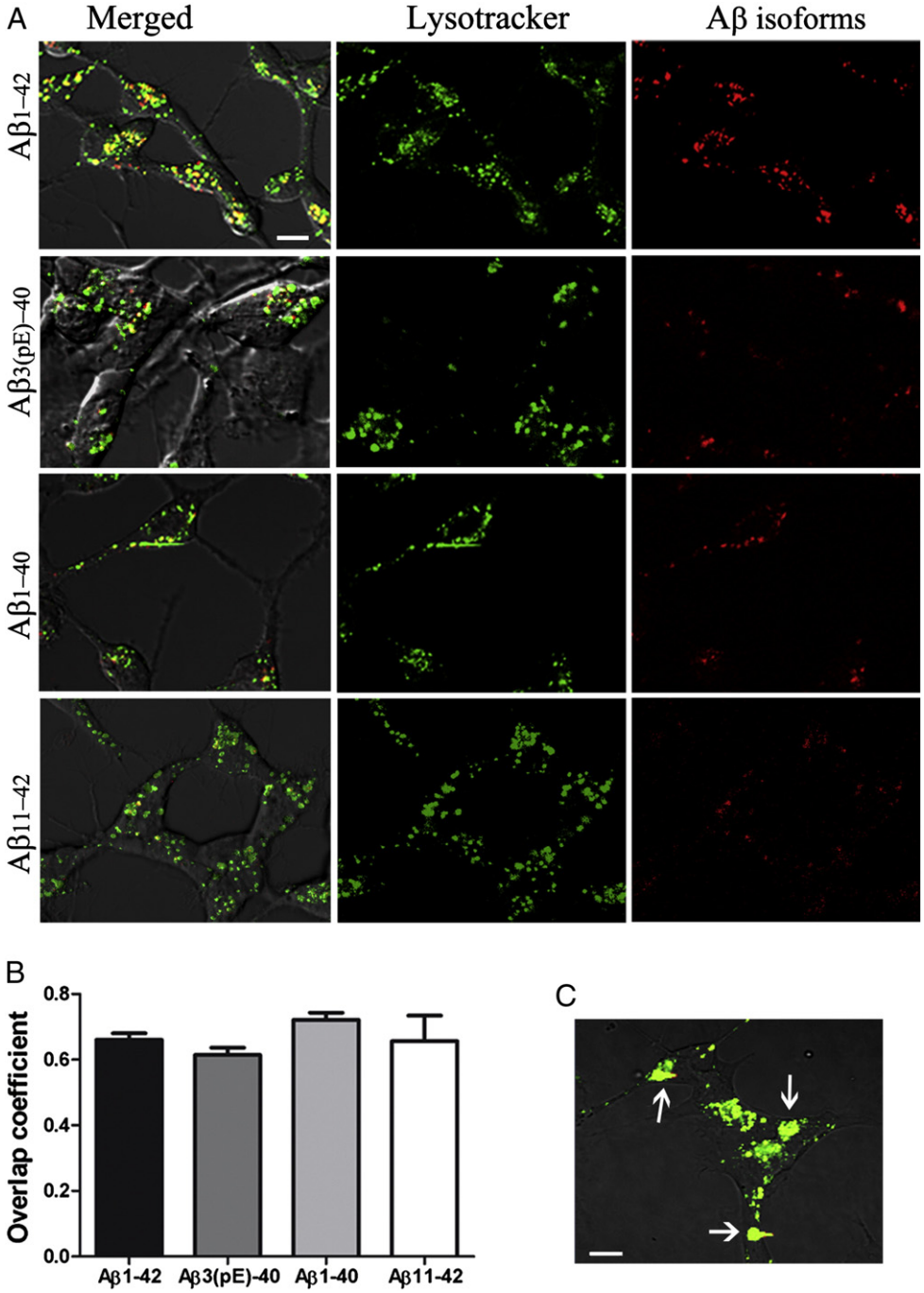

Fig. 4. Internalized Aβ co-localizes with lysosomes. (A) Superimposition of red, green and DIC confocal images shows oAβ-TMR isoforms (red), lysotracker-labeled late-endosomes/lysosomes (green) and co-localization (yellow) in differentiated SH-SY5Y cells. Images were taken after 3 h incubation of cells with 500 nM oAβ-TMR isoforms and thorough washing. Scale bar = 10 μm. (B) Mean overlap coefficients of co-localization of the oAβ isoforms (1–42, 3(pE)–40, 1–40 and 11–42) with lysotracker were calculated. No significant differences ($p > 0.05$, $n = 3$) were revealed (one-way ANOVA test). (C) Late-endosomes/lysosomes (green lysotracker) internalized with $oA\beta_{1-42}$ in donor cells showed the formation of extra-large vesicles over time (48 h shown). Arrows indicate oligomers internalized in extra-large late-endosomes/lysosomes. Scale bar = 5 μm; $n = 3$.

upregulation even after 72 h of internalization (Fig. 5E). Thus, the result suggests that lysosomal accumulation by degradation-resistant $oA\beta_{1-42}$TMR isoforms could induce intra-lysosomal stress-like behavior over time, while no similar effects were evident for more degradable Aβ isoforms.

Effects of monomers, dimers, oligomers and protofibrils of $A\beta_{1-42}$TMR on cell-to-cell transfer

The prepared oligomers of $A\beta_{1-42}$ TMR are a mixture of monomers, dimers and different sizes of other oligomers. To identify which of the species accumulate in the lysosome, the prepared oligomers were isolated using SEC (Fig. 6A). The purified monomers, dimers and oligomers showed considerable internalization in donor cells when donor cells were incubated with 500 nM of $A\beta_{1-42}$TMR species for 3 h. The dimers and oligomers were transferred from donor to acceptor cells, and purified monomers were also detected in cell-to-cell transfer. The extra-large lysosomes accumulated with $A\beta_{1-42}$TMR had significantly fewer monomers compared to oligomers and dimers in the transferred acceptor cells (Figs. 6B, C).

Furthermore, the effects of protofibrils were studied. The EM images showed that the prepared protofibrils of $A\beta_{1-42}$TMR are a mixture of

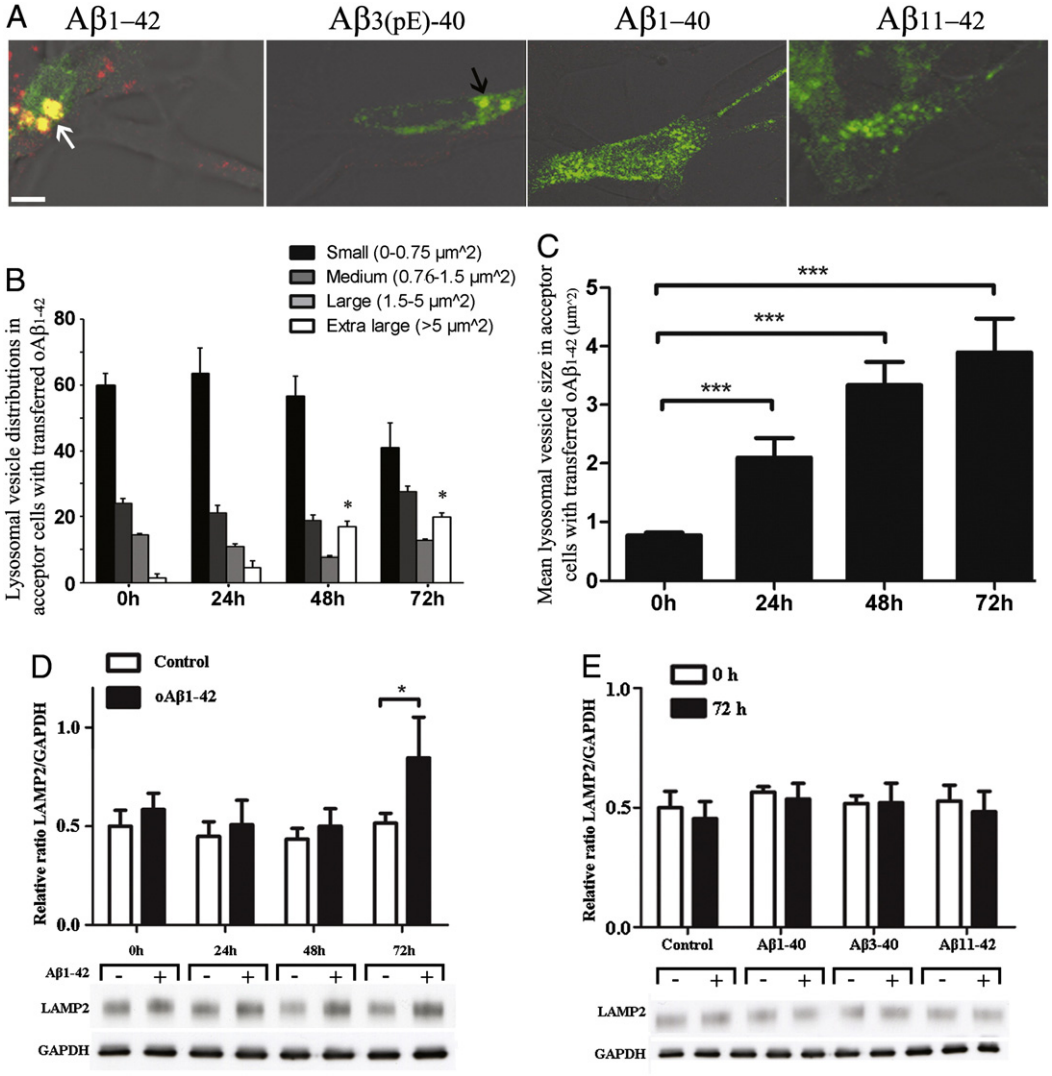

Fig. 5. Lysosomal alterations. The degradation resistance exhibited by oligomeric $A\beta_{1-42}$ induced a lysosomal stress-like behavior. (A) Confocal images showed the formation of abnormally extra-large lysosomal vesicles (white arrow) in the $A\beta_{1-42}$ transferred acceptor cells. While the other isoforms did not show extra-large lysosomes, a few medium- and large-sized lysosomes were visible in the $A\beta_{3(pE)-40}$ transferred acceptor cells (black arrow). Scale bar = 5 μm; n = 4. (B, C) Confocal images were analyzed, and the distributions (B) and mean sizes (C) of the lysosome vesicles were determined in acceptor cells subsequent to receiving $oA\beta_{1-42}$. Data were calculated from ~50 cells for each isoform and are represented as the means ± SD for distribution, but means ± SEM were used to represent mean size because of the vastly variable vesicle sizes; n = 6. (D) Quantification of lysosome-associated membrane protein 2 (LAMP-2) with Western blot revealed a significant increase after 72 h of $A\beta_{1-42}$ internalization in donor cells; n = 3. (E) Aβ isoforms 3(pE)–40, 1–40 and 11–42 did not show any significant increases in LAMP-2 expression after 72 h. The 0 h time point represents internalization of oAβ-TMR isoforms after 3 h incubation of donor cells with 1 μM oligomeric solutions and thorough washing; n = 3.

oligomers, protofibrils and fibrils (Fig. 6D). The prepared protofibrils disappeared significantly (85–91%) in donor cells after 48 h (Fig. 6E) and cell-to-cell transfer was significantly lower (17.2 ± 16%) than for the prepared oligomers (55.6 ± 7.8%) even at 24 h.

Neurotoxicity and mitochondrial membrane potential

It could be speculated that the release of oAβ leading to cell-to-cell transfer is caused by prior cell toxicity events. Thus, we investigated the effect of the different oAβ species on both cell viability and mitochondrial membrane stability and toxicity. An XTT assay was performed to determine the effect of oAβ isoforms on neuronal cell viability over time. The results did not reveal any significant difference in cell viability as measured by the XTT assay performed on donor cells having internalized 1 μM of any oAβ isoform over 72 h (Fig. 7A). Because the XTT assay reports cell death and/or mitochondrial toxicity, these data indicate that there was no significant cell death or mitochondrial toxicity upon the lysosomal accumulation of oAβ. Furthermore, the mitochondrial membrane potential was measured using a JC-1 assay. This assay did not show any significant mitochondrial toxicity at the time point (24 h) when transfer of oAβ was already abundant and abnormally large lysosomes had started to appear in donor and acceptor cells (Fig. 7B). We have previously reported the presence of organelle toxicities after longer periods of time with accumulated transferred $oA\beta_{1-42}$ (Nath et al., 2012). Together with the present results, the data suggest that cell-to-cell transfer is not secondary to cytotoxicity but that cellular transfer might be an early stress response by the cell to rid itself of intracellular, non-degradable, aggregation-prone accumulations.

Discussion

This study shows that different fluorescently labeled Aβ-isoforms (1–42, 1–40, 3(pE)–40 and 11–42) can transfer from one cell to another. Thus, cell-to-cell transfer is not dependent on a particular Aβ isoform, but the net amount of any isoform in the receiving cell is vastly variable because of differences in the capacity to clear and/or degrade these Aβ isoforms. Hence, insufficient clearance and/or degradation by cells create sizable intracellular accumulations of the $A\beta_{1-42}$ isoform, promoting

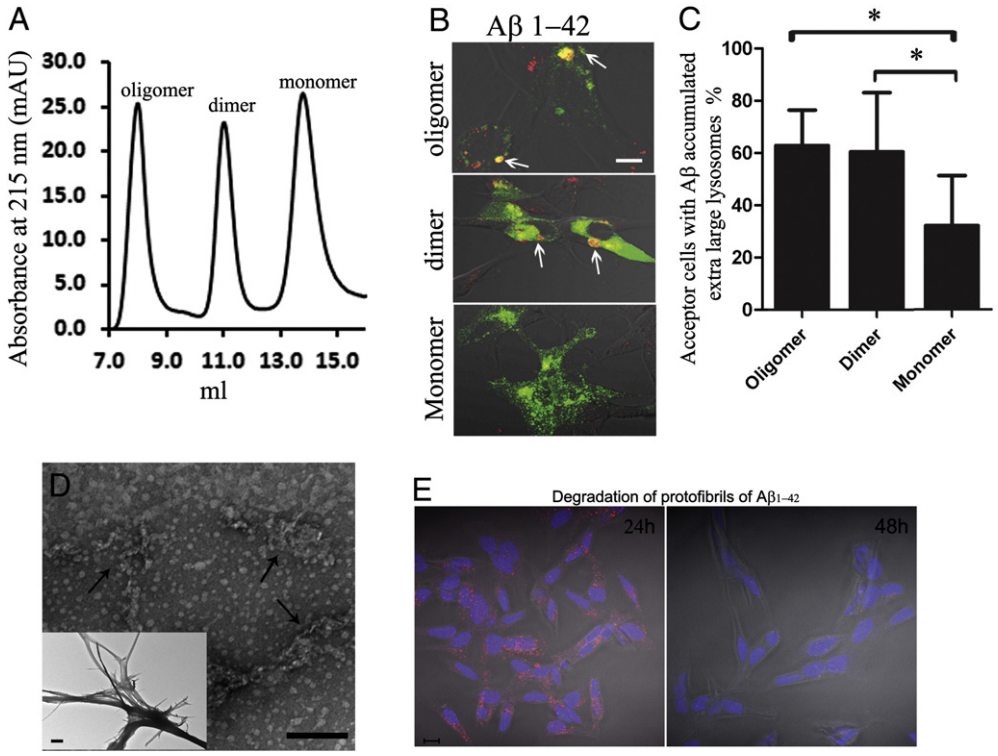

Fig. 6. Effects of monomers, dimers, oligomers and protofibrils of $A\beta_{1-42}$TMR on cell-to-cell transfer. (A) Separation of monomers, dimers and oligomers from the prepared $oA\beta_{1-42}$TMR by SEC; n = 3. (B) Formation of a high number of extra-large lysosomal vesicles (marked with white arrows) in dimers and oligomers of $oA\beta_{1-42}$TMR transferred acceptor cells after 48 h. Scale bar = 5 μm; n = 3. (C) Monomers of $A\beta_{1-42}$TMR formed significantly lower accumulations and significantly lower extra-large lysosome formations compared to dimers and oligomers; n = 3. (D) The EM images showed that the prepared protofibrils of $A\beta_{1-42}$TMR are a mixture of oligomers, protofibrils (black arrows) and fibrils. Scale bar = 200 nm. (E) The prepared protofibrils disappeared significantly (85–91%) in donor cells after 48 h. Scale bar = 10 μm. Data are calculated from ~50 cells for each isoform and are represented as the means ± SEM. Statistical significance was evaluated using a two-tailed unpaired Student's *t* test. *p < 0.05, **p < 0.01 and ***p < 0.001.

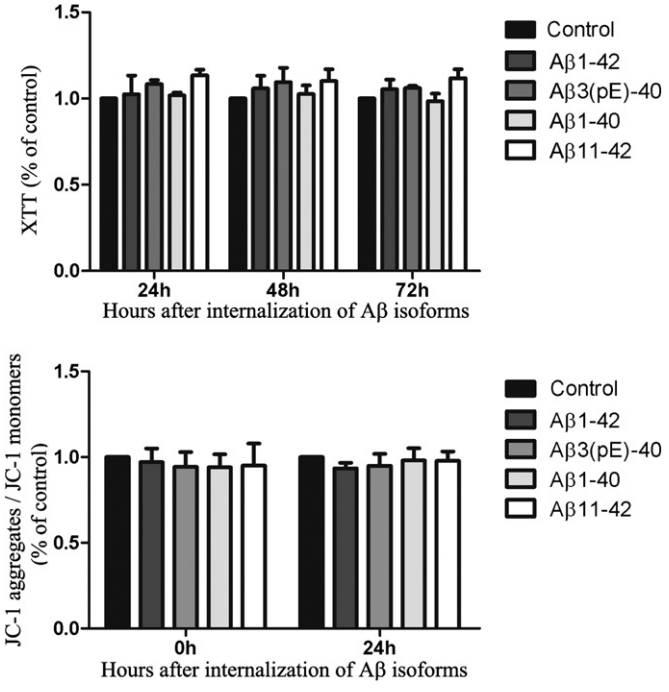

Fig. 7. Cytotoxicity. No cytotoxicity or mitochondrial toxicity was detected in donor cells internalized with 1 μm of the respective oligomeric isoforms over time. (A) No oligomeric isoform affected XTT processing compared to controls. (B) Mitochondrial potential was quantified with flow cytometry using a JC-1 assay, but no alterations were observed when comparing the Aβ-isoforms and the control. Data are represented as the means ± SD; n = 3.

the cell-to-cell transfer and making $A\beta_{1-42}$ a potentially toxic species. This study explains why the factors affecting clearance and/or degradation can have a strong impact on AD development.

Electron microscopic analysis of the oAβ preparations revealed that all isoforms were mainly oligomeric in structure. The results are consistent with previous reports showing that the $A\beta_{1-42}$ isoform propagates faster, forming larger-sized oligomers compared to the Aβ (1–40, 3(pE)–40, 11–42) isoforms (Ahmed et al., 2010). The characterizations of the oAβs and the effect of TMR tagging were performed in vitro; thus, their in vivo properties can only be inferred. However, we have previously shown similar cytotoxicity with both TMR-labeled and unlabeled $oA\beta_{1-42}$ (Nath et al., 2012). The oligomers of all of the oAβ-TMR isoforms were spontaneously internalized by neuronal cells from the extracellular space, accumulating mainly (65–85%) inside the late-endosomes/lysosomes immediately after internalization. Previous studies using $A\beta_{1-42}$ and $A\beta_{1-40}$ showed similar late-endosomal/lysosomal co-localization using lysotracker (Hu et al., 2009; Umeda et al., 2011). These data suggest that intracellular internalization from the extracellular space is independent of Aβ isoform, at least in a model using only partly differentiated cells.

Recent studies have reported the accumulation of Aβ peptides in lysosomes/endosomes (Zheng et al., 2011), endoplasmic reticulum and mitochondria (Umeda et al., 2011). The toxicity induced by Aβ from intracellular accumulation is starting to be accepted widely in the AD field (Gouras et al., 2010; LaFerla et al., 2007; Wirths et al., 2001). In our previous study, the accumulation of internalized $oA\beta_{1-42}$TMR from the extracellular space was observed in structures corresponding to vesicles of late-endosomes/lysosomes in both the donor and connector acceptor cells (Nath et al., 2012). In the present study, the accumulation of internalized $oA\beta_{1-42}$TMR in lysosomes over time resulted in abnormally

sized lysosomal vesicles in the donor and acceptor cells compared to lysosomes that had internalized more degradable isoforms, including oAβ_{11-42}TMR, oAβ_{1-40}TMR and oA$\beta_{3(PE)-40}$TMR. The increased expression of LAMP-2 with time in the donor cells after oAβ_{1-42}TMR internalization indicates the induction of cellular starvation and stress due to intra-lysosomal accumulations of non-degradable oAβ_{1-42}TMR. Interestingly, this lysosomal stress was not paralleled by mitochondria-associated toxicity at early time points, at least as revealed by the mitochondrial potential and XTT assays. Selective lysosomal toxicity in early AD-like pathology has been reported previously (Lee et al., 2011a). This result implies that cell-to-cell transfer is initiated before cytotoxicity develops. Longer periods of oAβ_{1-42} transfer have been shown to cause endosomal leakage and cytoskeletal damage (Nath et al., 2012). Thus, our results suggest that cellular transfer might be an early stress response by cells to get rid of intracellular, non-degradable, toxic accumulations. These results could also explain how seeds for AD pathology could pass on to new brain areas before the first cell starts to deteriorate.

Oligomers of different Aβ-isoforms (1–42, 1–40, 3(pE)–40 and 11–42) can all transfer from cell to cell. Thus, this transfer is not dependent on a particular Aβ isoform, but the net amount ending up in the receiving cell is vastly variable. There was a strong linear correlation between how well the cells were able to clear and/or degrade the respective oAβ and the number of connected acceptor cells containing transferred oAβ-TMRs. The aggregation-prone isoform oAβ_{1-42}TMR was found to transfer from donor cell to connected acceptor cells as previously shown (Nath et al., 2012), and the number of acceptor cells with transferred oligomers increased significantly over time. The oA$\beta_{3(pE)-40}$TMR isoform showed a partial resistance to clearance and/or degradation leading to moderate transfer as compared to the oAβ_{1-42}TMR isoform. This finding is in agreement with A$\beta_{3(pE)-40}$ alone being moderately toxic in AD pathology (Russo et al., 2002). However, adding oAβ_{1-40}TMR or oligomers of non-amyloidogenic oAβ_{11-42}TMR (Jang et al., 2013), both susceptible to clearance and/or degradation by cells, to donor cells resulted in insignificant accumulation in and insignificant transfer to the connected acceptor cells. The latter finding is consistent with oAβ_{11-42}TMR only showing some toxic properties when modified at the N-terminal amino acid with pyroglutamate (Jang et al., 2010, 2013). As in the different Aβ-isoform oligomers, the isolated monomers, dimers and oligomers from the oAβ_{1-42}TMR also participated in cell-to-cell transfer according to their lysosomal accumulations. Purified monomers and dimers are highly unstable and can propagate further to form higher oligomers. Monomers are not neurotoxic, and the monomer-to-dimer transition is a slow process that happens only under certain favorable environments (Nag et al., 2011). However, dimers have been reported to be potential seeds that accelerate propagation to form higher aggregates (Shankar et al., 2008). Thus, the lag phase for the aggregation process should be longer for monomers, and the monomeric Aβ will be more susceptible to degradation compared to the dimers and oligomers. As a result, less accumulation will occur with comparatively slower aggregating monomeric species. In concert with the findings for the other degradable isoforms, including oAβ_{1-40} and oAβ_{11-42}, oAβ_{1-42}, monomers have a lower net transfer, and the formation of extra-large lysosome vesicles is significantly lower. Because only the net remaining Aβ can cause seeding and pathology in the acceptor cells, these results may explain why the aggregation-prone and less degradable oAβ_{1-42} is a highly toxic species. The profibrils of Aβ_{1-42}, which were prepared differently from the oligomers, consisted of a mixture of oligomers, protofibrils and fibrils. Fibrillization of Aβ_{1-42} is a progressive process and separation of a distinct stable form is technically difficult. The faster disappearance kinetics of protofibrils compared to oligomers might explain the variable stability with stochastically induced seeds produced differently.

Recent studies of other neurodegenerative non-prion proteins (e.g., tau, α-synuclein, huntingtin, etc.) have revealed similar cell-to-cell propagation and prion-like pathology progression (Brundin et al., 2010; Lee et al., 2010). Together, these studies and our data support the possibility of similar, prion-like propagation in different neurodegenerative diseases (see Prusiner, 2012 for a review). Consistent with this suggestion, recent studies on transgenic mice and primate models showed the induction of Aβ aggregation and propagation of AD pathology from both injected AD brain extracts (Meyer-Luehmann et al., 2006; Ridley et al., 2006) and synthetic Aβ (Jucker and Walker, 2013; Stohr et al., 2012). However, not all of these studies have been able to show the induction of propagation by synthetic Aβ (Meyer-Luehmann et al., 2006). Fibrils formed by synthetic Aβ are sensitive to protease degradation and rarely show seeding capacity (Langer et al., 2011). Injecting rodent Aβ seeds into wild type mice also failed to induce pathology propagation. Rather, propagation seems to depend on the source of the exogenous Aβ seeds in transgenic animal models (reviewed in Jucker and Walker, 2013). However, unlike Aβ, tauopathy and α-synucleinopathy can induce pathology from exogenous seeds in wild-type mice (reviewed in Jucker and Walker, 2013). In vitro, Aβ forms polymorphic amyloid aggregates. In contrast a recent study by Lu et al. (2013) showed the existence of individually distinct Aβ fibril conformations in AD patients, depending on the type of AD pathology found. These results imply that the stochastically induced multiple nucleated seeds in vivo could have been eliminated by amyloid clearance mechanisms. However, individuals with decreased clearance efficiency could have failed to degrade a particular type of seeds leading to propagation of pathology with distinct Aβ fibril conformations (Lu et al., 2013), similar to the results seen in our study. In the human brain, degradation and clearance of toxic products such as non-degradable seeds are accomplished by neurons in concert with glial cells. Therefore, intracellular accumulations and their progression from small amounts of non-degradable seeds may take years before causing pathology.

Conclusion

The progressions of toxic seeds of Aβ to connected cells and their catalyzing effect to induce further aggregates, similar to the pathology observed with prions, have been addressed in several studies (Nussbaum et al., 2012; Stohr et al., 2012). The role of Aβ seeds in nucleation and aggregation is a well-established fact, but the prion theory for pathology propagation ignores many other influencing factors in the AD etiology (Lahiri, 2012). Many of these factors influence cellular clearance or degradation systems and have a strong influence on AD pathology. These factors include dietary cholesterol, metabolic disorders, ApoE lipoprotein, low-density lipoprotein receptors and insufficient lysosomal–proteosomal and insulin-degrading enzymes (Selkoe, 1997). Hence, the strong correlation between failed clearance and/or degradation with subsequent intracellular accumulation and cell-to-cell propagation revealed in this study can explain how the prion model for AD progression can act together with factors that influence cellular clearance or degradation systems in the development of AD.

Acknowledgment

This research was made possible by funding from the Swedish Alzheimer's Foundation, the Hans-Gabriel and Alice Trolle-Wachtmeisters Foundation for Medical Research, the Gustav V and Queen Victoria's Foundation, the Swedish Dementia Foundation, the Linköping University Neurobiology Center and the Östergötland County Council.

References

Agholme, L., Lindstrom, T., Kagedal, K., Marcusson, J., Hallbeck, M., 2010. An in vitro model for neuroscience: differentiation of SH-SY5Y cells into cells with morphological and biochemical characteristics of mature neurons. J. Alzheimers Dis. 20, 1069–1082.

Agholme, L., Hallbeck, M., Benedikz, E., Marcusson, J., Kagedal, K., 2012. Amyloid-beta secretion, generation, and lysosomal sequestration in response to proteasome inhibition: involvement of autophagy. J. Alzheimers Dis. 31, 343–358.

Ahmed, M., Davis, J., Aucoin, D., Sato, T., Ahuja, S., Aimoto, S., Elliott, J.I., Van Nostrand, W.E., Smith, S.O., 2010. Structural conversion of neurotoxic amyloid-beta(1–42) oligomers to fibrils. Nat. Struct. Mol. Biol. 17, 561–567.

Bains, M., Heidenreich, K.A., 2009. Live-cell imaging of autophagy induction and autophagosome–lysosome fusion in primary cultured neurons. Methods Enzymol. 453, 145–158.
Benilova, I., Karran, E., De Strooper, B., 2012. The toxic Abeta oligomer and Alzheimer's disease: an emperor in need of clothes. Nat. Neurosci. 15, 349–357.
Brouillette, J., Caillierez, R., Zommer, N., Alves-Pires, C., Benilova, I., Blum, D., De Strooper, B., Buee, L., 2012. Neurotoxicity and memory deficits induced by soluble low-molecular-weight amyloid-beta1–42 oligomers are revealed in vivo by using a novel animal model. J. Neurosci. 32, 7852–7861.
Brundin, P., Melki, R., Kopito, R., 2010. Prion-like transmission of protein aggregates in neurodegenerative diseases. Nat. Rev. Mol. Cell Biol. 11, 301–307.
Clavaguera, F., Bolmont, T., Crowther, R.A., Abramowski, D., Frank, S., Probst, A., Fraser, G., Stalder, A.K., Beibel, M., Staufenbiel, M., Jucker, M., Goedert, M., Tolnay, M., 2009. Transmission and spreading of tauopathy in transgenic mouse brain. Nat. Cell Biol. 11, 909–913.
Cuervo, A.M., Dice, J.F., 2000. Regulation of lamp2a levels in the lysosomal membrane. Traffic 1, 570–583.
Deane, R., Sagare, A., Hamm, K., Parisi, M., Lane, S., Finn, M.B., Holtzman, D.M., Zlokovic, B.V., 2008. ApoE isoform-specific disruption of amyloid β peptide clearance from mouse brain. J. Clin. Invest. 118, 4002–4013.
Desplats, P., Lee, H.J., Bae, E.J., Patrick, C., Rockenstein, E., Crews, L., Spencer, B., Masliah, E., Lee, S.J., 2009. Inclusion formation and neuronal cell death through neuron-to-neuron transmission of alpha-synuclein. Proc. Natl. Acad. Sci. U. S. A. 106, 13010–13015.
Gouras, G.K., Tampellini, D., Takahashi, R.H., Capetillo-Zarate, E., 2010. Intraneuronal beta-amyloid accumulation and synapse pathology in Alzheimer's disease. Acta Neuropathol. 119, 523–541.
Hardy, J., Selkoe, D.J., 2002. The amyloid hypothesis of Alzheimer's disease: progress and problems on the road to therapeutics. Science 297, 353–356.
Haugland, R.P., 2001. Antibody conjugates for cell biology. Curr. Protoc. Cell Biol. (Chapter 16:Unit 16. 15).
Hu, X., Crick, S.L., Bu, G., Frieden, C., Pappu, R.V., Lee, J.M., 2009. Amyloid seeds formed by cellular uptake, concentration, and aggregation of the amyloid-beta peptide. Proc. Natl. Acad. Sci. U. S. A. 106, 20324–20329.
Jang, H., Arce, F.T., Ramachandran, S., Capone, R., Azimova, R., Kagan, B.L., Nussinov, R., Lal, R., 2010. Truncated beta-amyloid peptide channels provide an alternative mechanism for Alzheimer's disease and Down syndrome. Proc. Natl. Acad. Sci. U. S. A. 107, 6538–6543.
Jang, H., Connelly, L., Arce, F.T., Ramachandran, S., Lal, R., Kagan, B.L., Nussinov, R., 2013. Alzheimer's disease: which type of amyloid-preventing drug agents to employ? Phys. Chem. Chem. Phys. 15, 8868–8877.
Jucker, M., Walker, L.C., 2013. Self-propagation of pathogenic protein aggregates in neurodegenerative diseases. Nature 501, 45–51.
Klein, W.L., Krafft, G.A., Finch, C.E., 2001. Targeting small Abeta oligomers: the solution to an Alzheimer's disease conundrum? Trends Neurosci. 24, 219–224.
Klingstedt, T., Aslund, A., Simon, R.A., Johansson, L.B., Mason, J.J., Nystrom, S., Hammarstrom, P., Nilsson, K.P., 2011. Synthesis of a library of oligothiophenes and their utilization as fluorescent ligands for spectral assignment of protein aggregates. Org. Biomol. Chem. 9, 8356–8370.
Kuperstein, I., Broersen, K., Benilova, I., Rozenski, J., Jonckheere, W., Debulpaep, M., Vandersteen, A., Segers-Nolten, I., Van Der Werf, K., Subramaniam, V., Braeken, D., Callewaert, G., Bartic, C., D'Hooge, R., Martins, I.C., Rousseau, F., Schymkowitz, J., De Strooper, B., 2010. Neurotoxicity of Alzheimer's disease Abeta peptides is induced by small changes in the Abeta42 to Abeta40 ratio. EMBO J. 29, 3408–3420.
LaFerla, F.M., Green, K.N., Oddo, S., 2007. Intracellular amyloid-beta in Alzheimer's disease. Nat. Rev. Neurosci. 8, 499–509.
Lahiri, D.K., 2012. Prions: a piece of the puzzle? Science 337, 1172.
Langer, F., Eisele, Y.S., Fritschi, S.K., Staufenbiel, M., Walker, L.C., Jucker, M., 2011. Soluble Abeta seeds are potent inducers of cerebral beta-amyloid deposition. J. Neurosci. 31, 14488–14495.
Lee, S.J., Desplats, P., Sigurdson, C., Tsigelny, I., Masliah, E., 2010. Cell-to-cell transmission of non-prion protein aggregates. Nat. Rev. Neurol. 6, 702–706.
Lee, S., Sato, Y., Nixon, R.A., 2011a. Lysosomal proteolysis inhibition selectively disrupts axonal transport of degradative organelles and causes an Alzheimer's-like axonal dystrophy. J. Neurosci. 31, 7817–7830.
Lee, S., Sato, Y., Nixon, R.A., 2011b. Primary lysosomal dysfunction causes cargo-specific deficits of axonal transport leading to Alzheimer-like neuritic dystrophy. Autophagy 7, 1562–1563.
Lu, J.X., Qiang, W., Yau, W.M., Schwieters, C.D., Meredith, S.C., Tycko, R., 2013. Molecular structure of beta-amyloid fibrils in Alzheimer's disease brain tissue. Cell 154, 1257–1268.
Meyer-Luehmann, M., Coomaraswamy, J., Bolmont, T., Kaeser, S., Schaefer, C., Kilger, E., Neuenschwander, A., Abramowski, D., Frey, P., Jaton, A.L., Vigouret, J.M., Paganetti, P., Walsh, D.M., Mathews, P.M., Ghiso, J., Staufenbiel, M., Walker, L.C., Jucker, M., 2006. Exogenous induction of cerebral beta-amyloidogenesis is governed by agent and host. Science 313, 1781–1784.
Nag, S., Sarkar, B., Bandyopadhyay, A., Sahoo, B., Sreenivasan, V.K., Kombrabail, M., Muralidharan, C., Maiti, S., 2011. Nature of the amyloid-beta monomer and the monomer–oligomer equilibrium. J. Biol. Chem. 286, 13827–13833.
Nath, S., Agholme, L., Kurudenkandy, F.R., Granseth, B., Marcusson, J., Hallbeck, M., 2012. Spreading of neurodegenerative pathology via neuron-to-neuron transmission of beta-amyloid. J. Neurosci. 32, 8767–8777.
Nixon, R.A., Yang, D.S., Lee, J.H., 2008. Neurodegenerative lysosomal disorders: a continuum from development to late age. Autophagy 4, 590–599.
Nussbaum, J.M., Schilling, S., Cynis, H., Silva, A., Swanson, E., Wangsanut, T., Tayler, K., Wiltgen, B., Hatami, A., Ronicke, R., Reymann, K., Hutter-Paier, B., Alexandru, A., Jagla, W., Graubner, S., Glabe, C.G., Demuth, H.U., Bloom, G.S., 2012. Prion-like behaviour and tau-dependent cytotoxicity of pyroglutamylated amyloid-beta. Nature 485, 651–655.
Prusiner, S.B., 2012. Cell biology. A unifying role for prions in neurodegenerative diseases. Science 336, 1511–1513.
Ridley, R.M., Baker, H.F., Windle, C.P., Cummings, R.M., 2006. Very long term studies of the seeding of beta-amyloidosis in primates. J. Neural Transm. 113, 1243–1251.
Roehm, N.W., Rodgers, G.H., Hatfield, S.M., Glasebrook, A.L., 1991. An improved colorimetric assay for cell proliferation and viability utilizing the tetrazolium salt XTT. J. Immunol. Methods 142, 257–265.
Russo, C., Violani, E., Salis, S., Venezia, V., Dolcini, V., Damonte, G., Benatti, U., D'Arrigo, C., Patrone, E., Carlo, P., Schettini, G., 2002. Pyroglutamate-modified amyloid beta-peptides – AbetaN3(pE) – strongly affect cultured neuron and astrocyte survival. J. Neurochem. 82, 1480–1489.
Saftig, P., Eskelinen, E.L., 2008. Live longer with LAMP-2. Nat. Med. 14, 909–910.
Scudiero, D.A., Shoemaker, R.H., Paull, K.D., Monks, A., Tierney, S., Nofziger, T.H., Currens, M.J., Seniff, D., Boyd, M.R., 1988. Evaluation of a soluble tetrazolium/formazan assay for cell growth and drug sensitivity in culture using human and other tumor cell lines. Cancer Res. 48, 4827–4833.
Selkoe, D.J., 1997. Alzheimer's disease: genotypes, phenotypes, and treatments. Science 275, 630–631.
Selkoe, D.J., 2008. Soluble oligomers of the amyloid beta-protein impair synaptic plasticity and behavior. Behav. Brain Res. 192, 106–113.
Shankar, G.M., Li, S., Mehta, T.H., Garcia-Munoz, A., Shepardson, N.E., Smith, I., Brett, F.M., Farrell, M.A., Rowan, M.J., Lemere, C.A., Regan, C.M., Walsh, D.M., Sabatini, B.L., Selkoe, D.J., 2008. Amyloid-beta protein dimers isolated directly from Alzheimer's brains impair synaptic plasticity and memory. Nat. Med. 14, 837–842.
Stohr, J., Watts, J.C., Mensinger, Z.L., Oehler, A., Grillo, S.K., Dearmond, S.J., Prusiner, S.B., Giles, K., 2012. Purified and synthetic Alzheimer's amyloid beta (Abeta) prions. Proc. Natl. Acad. Sci. U. S. A. 109, 11025–11030.
Tekirian, T.L., Yang, A.Y., Glabe, C., Geddes, J.W., 1999. Toxicity of pyroglutaminated amyloid beta-peptides 3(pE)–40 and –42 is similar to that of A beta1–40 and –42. J. Neurochem. 73, 1584–1589.
Umeda, T., Tomiyama, T., Sakama, N., Tanaka, S., Lambert, M.P., Klein, W.L., Mori, H., 2011. Intraneuronal amyloid beta oligomers cause cell death via endoplasmic reticulum stress, endosomal/lysosomal leakage, and mitochondrial dysfunction in vivo. J. Neurosci. Res. 89, 1031–1042.
Villeda, S.A., Luo, J., Mosher, K.I., Zou, B., Britschgi, M., Bieri, G., Stan, T.M., Fainberg, N., Ding, Z., Eggel, A., Lucin, K.M., Czirr, E., Park, J.S., Couillard-Despres, S., Aigner, L., Li, G., Peskind, E.R., Kaye, J.A., Quinn, J.F., Galasko, D.R., Xie, X.S., Rando, T.A., Wyss-Coray, T., 2011. The ageing systemic milieu negatively regulates neurogenesis and cognitive function. Nature 477, 90–94.
Wirths, O., Multhaup, G., Czech, C., Blanchard, V., Moussaoui, S., Tremp, G., Pradier, L., Beyreuther, K., Bayer, T.A., 2001. Intraneuronal Abeta accumulation precedes plaque formation in beta-amyloid precursor protein and presenilin-1 double-transgenic mice. Neurosci. Lett. 306, 116–120.
Zheng, L., Terman, A., Hallbeck, M., Dehvari, N., Cowburn, R.F., Benedikz, E., Kagedal, K., Cedazo-Minguez, A., Marcusson, J., 2011. Macroautophagy-generated increase of lysosomal amyloid beta-protein mediates oxidant-induced apoptosis of cultured neuroblastoma cells. Autophagy 7, 1528–1545.